Eur J Vasc Endovasc Surg (2008) **36**, 668–676

Patient-Specific AAA Wall Stress Analysis: 99-Percentile Versus Peak Stress

L. Speelman [a,*], E.M.H. Bosboom [b], G.W.H. Schurink [c], F.A.M.V.I. Hellenthal [c], J. Buth [d], M. Breeuwer [e], M.J. Jacobs [c], F.N. van de Vosse [a]

[a] *Eindhoven University of Technology, Department of Biomedical Engineering, The Netherlands*
[b] *Maastricht University Medical Center, Department of Biomedical Engineering, The Netherlands*
[c] *Maastricht University Medical Center, Department of General Surgery, The Netherlands*
[d] *Catharina Hospital Eindhoven, Department of Vascular Surgery, The Netherlands*
[e] *Philips Medical Center, Department of Clinical and Healthcare Informatics, The Netherlands*

Submitted 17 July 2008; accepted 13 September 2008
Available online 11 October 2008

KEYWORDS
Abdominal aortic aneurysm;
AAA wall stress analysis;
Rupture risk analysis

Abstract *Objective:* Biomechanically, rupture of an Abdominal Aortic Aneurysm (AAA) occurs when the stress acting on the wall due to the blood pressure, exceeds the strength of the wall. Peak wall stress estimations, based on CT reconstruction, may be prone to observer variation. This study focuses on the robustness and reproducibility of AAA wall stress assessment and the relation with geometrical features of the AAA.
Methods: The AAAs of twenty patients were reconstructed by three operators. Both the peak and 99-percentile stress were used for intra- and inter-operator variability using the intraclass correlation coefficient (ICC). A regression analysis was performed to relate the stress parameters with the maximum diameter. Outliers were analyzed by their geometrical characteristics.
Results: The intra-operator ICC was 0.73–0.79 for the peak stress and 0.94 for the 99-percentile stress. The inter-operator ICC was 0.71 for the peak stress and 0.95 for the 99-percentile stress. A significant linear relation with the diameter was found only for the 99-percentile stress.
Conclusions: The 99-percentile stress is more reproducible than peak wall stress. A significant relation between wall stress and diameter was found. Other geometrical features had no statistical relation with high stress.

* Corresponding author. L. Speelman, azM, Department of Biomedical Engineering, PO Box 5800, 6202 AZ Maastricht, The Netherlands. Tel.: +31 43 3876291; fax: +31 43 3874277.
E-mail address: l.speelman@tue.nl (L. Speelman).

1078-5884/$34
doi:10.1016/j.ejvs.2008.09.007

Introduction

The current criterion for abdominal aortic aneurysm (AAA) operative repair is an anterior–posterior diameter of the AAA of at least 5.5 cm.[1] Statistically, the risk of rupture is than found to be equal to the risk of the repair procedure. In the past, several studies have concluded that the diameter may not be reliable as rupture risk criterion and that it should be replaced by a more patient-specific criterion.[2–4] Therefore, multiple studies have focused on patient-specific wall stress analyses.[5–8] Fillinger et al. studied the differences in peak wall stress between patients with elective and symptomatic or ruptured AAAs (mean AAA diameter 6.6 cm) and found that peak wall stresses were significantly higher for the latter group.[5] Truijers et al. computed peak wall stress in small ruptured and asymptomatic AAAs and concluded that the wall stress at maximum systolic blood pressure was significantly higher for the ruptured group.[8] Before wall stress can be used as risk parameter on a patient-specific basis, wall stress analysis software needs to be evaluated on reproducibility and clinical applicability.

For the calculation of AAA wall stress, the AAA geometry is reconstructed from medical images, in most cases Computed Tomographic Angiography (CTA). Accurate depiction of the AAA surface contour and shape by CTA reconstructive techniques requires a complex segmentation technique to reassemble adjacent axial slices, smooth surface transitions between slices, maintain longitudinal orientation relative to the centerline, and accurately reproduce the relative tortuosity present in vivo. Manual, user-generated segmentation has been shown to be time-consuming and leads to greater differences in derived wall stresses because of variability in AAA shapes created by different users.[9] Automation of segmentation may reduce shape-induced stress variability due to the standardized smoothing and contouring steps in the procedure.

Recently, the first study on reliability of AAA wall stress analyses was published by Heng et al.[9] Segmentation of the AAAs was performed by manual contour selection in each CT-slice. For the inter-operator variation, the percentage of average deviation from the mean peak wall stress varied from 5% to 24%. However, the maximum deviation between two peak stresses for models of the same patient was found up to 100%.[9] A double analysis on 10 patients by one operator resulted in differences up to 40%. The small variations in geometry, introduced by the manual segmentation thus have a strong effect on the peak wall stress.

The aim of this study is two-fold: (1) to evaluate the robustness and reproducibility of AAA wall stress assessment and (2) to relate wall stress with geometrical parameters of the AAA. It may be expected that the stress relates to the diameter, as the diameter has proven to be a relatively good indicator of the rupture rate. Other geometrical features may additionally influence the level of wall stress.

Since peak wall stress is found to be strongly dependent on local geometrical irregularities,[9] also percentiles stress are considered in the analysis. The 99-percentile stress is defined as the peak stress value in the AAA after exclusion of 1% of the total surface area with the highest stresses.[10] This way, the absolute peak stress, possibly influenced by small geometrical variations, is excluded from the analysis. For the robustness and reproducibility, intra- and inter-operator variations are determined for the peak and 99-percentile wall stresses between three operators and CT-data from 20 patients.

Materials and Methods

The contrast-enhanced CT scans of the AAAs of 20 patients were obtained from the University Medical Center Maastricht (The Netherlands, $n = 11$) and the Catharina Hospital in Eindhoven (The Netherlands, $n = 9$). The CT scans are performed in the arterial phase, with an in-plane resolution of 512×512 pixels and a slice-thickness of either 1 or 2 mm (due to the use of different CT-scanners in the two hospitals). Brachial systolic, diastolic and mean arterial pressures (SP, DP and MAP) were recorded for all patients within 30 min after the CT scan using a Dynamap 1846SX/P (Critikon Inc., Tampa, FL, USA). The medical history and demographics for each patient was obtained. Research approval was given by the local Medical Ethics Commissions of the hospitals involved. All patients signed informed consent.

Segmentation and mesh creation

Software developed by Philips Medical Systems (Best, The Netherlands) was used to automatically segment the AAA from the CT scan.[10,11] The required user-input includes selecting a starting point proximal to the AAA and two end points, distal to the aortic bifurcation. Then, based on the Hounsfield values of the three user points, the centerline of the AAA was tracked automatically. Based on the centerline, a 3D active object (3DAO) was used to automatically detect the edges of the lumen and the AAA wall (Fig. 1). The 3DAO implementation is based on work by Delingette[12] and has been previously used for segmentation of vascular structures, including AAAs.[11,13,14] Visual inspection of the 3DAO was done and manual corrections were made to the 3D surface by changing slice contours, where the user judges that the automatic segmentation is inaccurate (Fig. 2).

The segmentation of the AAA wall was used as input for the wall stress simulations. The aortic bifurcation was excluded from the segmentation in case the iliac arteries were so strongly angulated, calcified or stenotic that segmentation was impossible.

AAA wall stress analysis

The commercially available finite element software Sepran (Sepra, Delft, The Netherlands) was used to calculate the AAA wall stresses. A constant wall thickness of 2 mm was applied and an incompressible isotropic hyper-elastic material model (shear modulus of 0.9 MPa) was used for the AAA wall. A mesh typically consisted of approximately 30,000 quadratic 15-node tetrahedral elements. A mesh refinement study was performed prior to the study and mesh independence was reached at this element-size. The patient group averaged systolic blood pressure is applied to

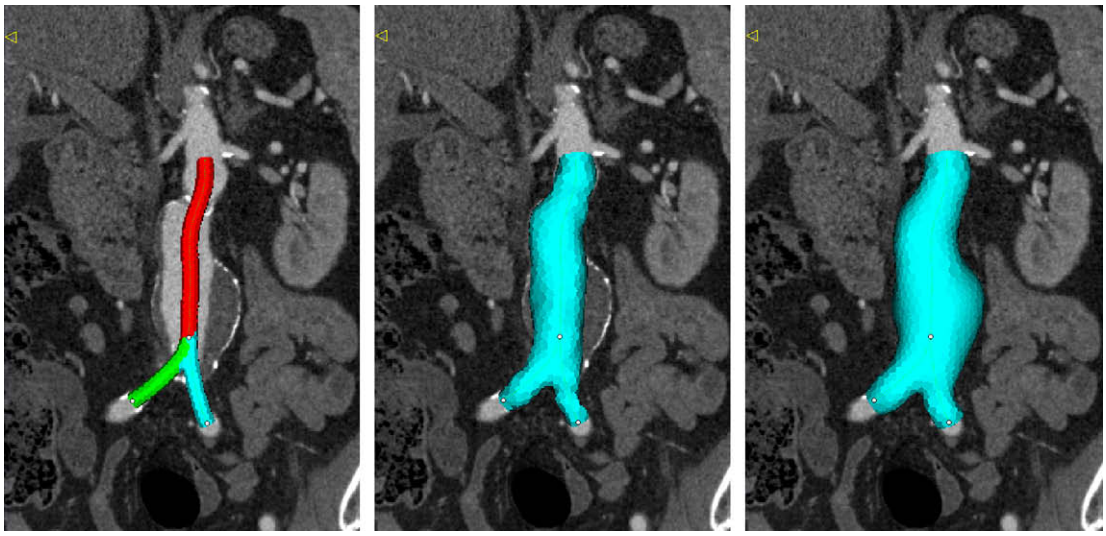

Figure 1 The 3D active object of the centerline (left), the lumen (middle) and the AAA wall (right).

the inner wall of the model in increasing iterative steps. In each step equilibrium between the applied pressure and wall stresses and corresponding deformations is computed. The computations are based on element-wise local and hereby global conservation of mass and momentum (second law of Newton) by subdividing the aneurysm wall in a finite number of small elements. Boundary conditions are required to solve the finite element system, therefore, in addition to the prescribed pressure, the most distal and proximal planes of the models are constrained in all directions.

Local stresses, strains and displacements were calculated. In each node, maximum principal stress is computed as a single stress measure. The peak wall stress was determined by computing the highest stress in the mesh. The 99-percentile stress was computed by excluding 1% of all nodes containing the highest stress. Since all elements have the same size, this corresponds to 1% of the surface area. Thereafter, the highest stress of the remaining nodes is defined as the 99-percentile stress.[10]

Study design

Three operators assessed all 20 patients, of which two operators each performed the analysis 5 times per patient (operator 1 and 2). Operator 1 has in-depth knowledge about the segmentation and wall stress computation procedures and is experienced with interpreting CT-data from AAA patients, whereas operator 2 has no knowledge of the procedures and no experience with interpreting CT-data. All segmentations of the same AAA were made within a three-week period and no blinding or scrambling of the CT-data was performed, as the operators could identify the patients by the AAA characteristics, because of the relative small patient group. Operator 3 is highly experienced with interpreting CT-data but has no knowledge about the

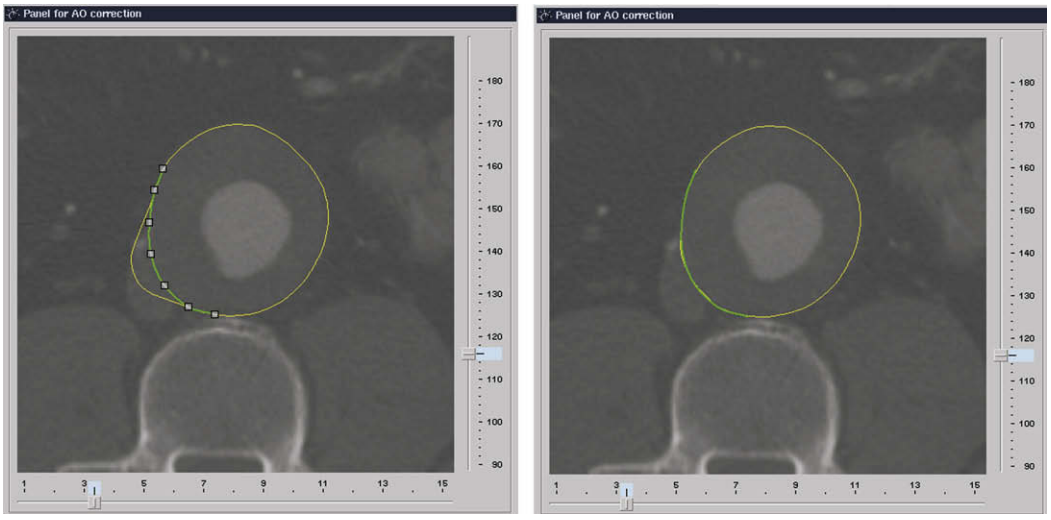

Figure 2 Left: Failure of the automatic segmentation into the vena cava (thin solid line) and manual corrected contour (solid dotted line). Right: Corrected contour.

Table 1 Patient demographics

Demographics	Value
Age (mean (range))	72 (59—83)
Gender (M/F)	16/4
Smoking (%)	15
Drug controlled hypertension (%)	80
Ischemic heart disease (%)	50
COPD (%)	30
Blood pressure (mean SP/DP/MAP)	140/90/105 mmHg
Maximum AP diameter (mean(range))	49 (44—57)

computational procedures. On forehand, it was agreed to choose the starting point just distal to the ostia of the most proximal renal artery and the two end points a few centimeters distal to the aortic bifurcation, where curvature of the iliac arteries is minimum. Manual adaptation of the 3DAO was performed based on personal insight of each operator.

Data analysis

For the statistical analysis, Statgraphics Centurion XV (StatPoint, Herndon, Virginia, USA) was used. Intra-operator variation was computed by the intraclass correlation coefficient (ICC). To evaluate a possible learning effect, absolute difference in peak and 99-percentile stress between the first and second segmentation is compared to the difference between the last and second last segmentation. Bland—Altman plots were made and inter-operator ICC was computed. A simple regression analysis was performed to relate peak and 99-percentile stress with the maximum anterior—posterior diameter of the AAA. The outlier peak stress values observed with different AAA geometrical characteristics were compared. One of the geometric variables that may influence the risk of rupture is tortuosity of the aneurysm.[15—17] Therefore the tortuosities of the central flow line (CFL) and the central lumen line (CLL) are evaluated. The lumen is defined as the volume within the AAA wall, thus including intraluminal thrombus. The tortuosity of the CLL and CFL is computed by dividing the distance along the central line between the lowest renal artery and the aortic bifurcation by the straight-line distance between these points.[16]

Results

The demographics of the patients are displayed in Table 1. Our patient group represents a typical sample selection from the population that suffers from an AAA.[8,9]

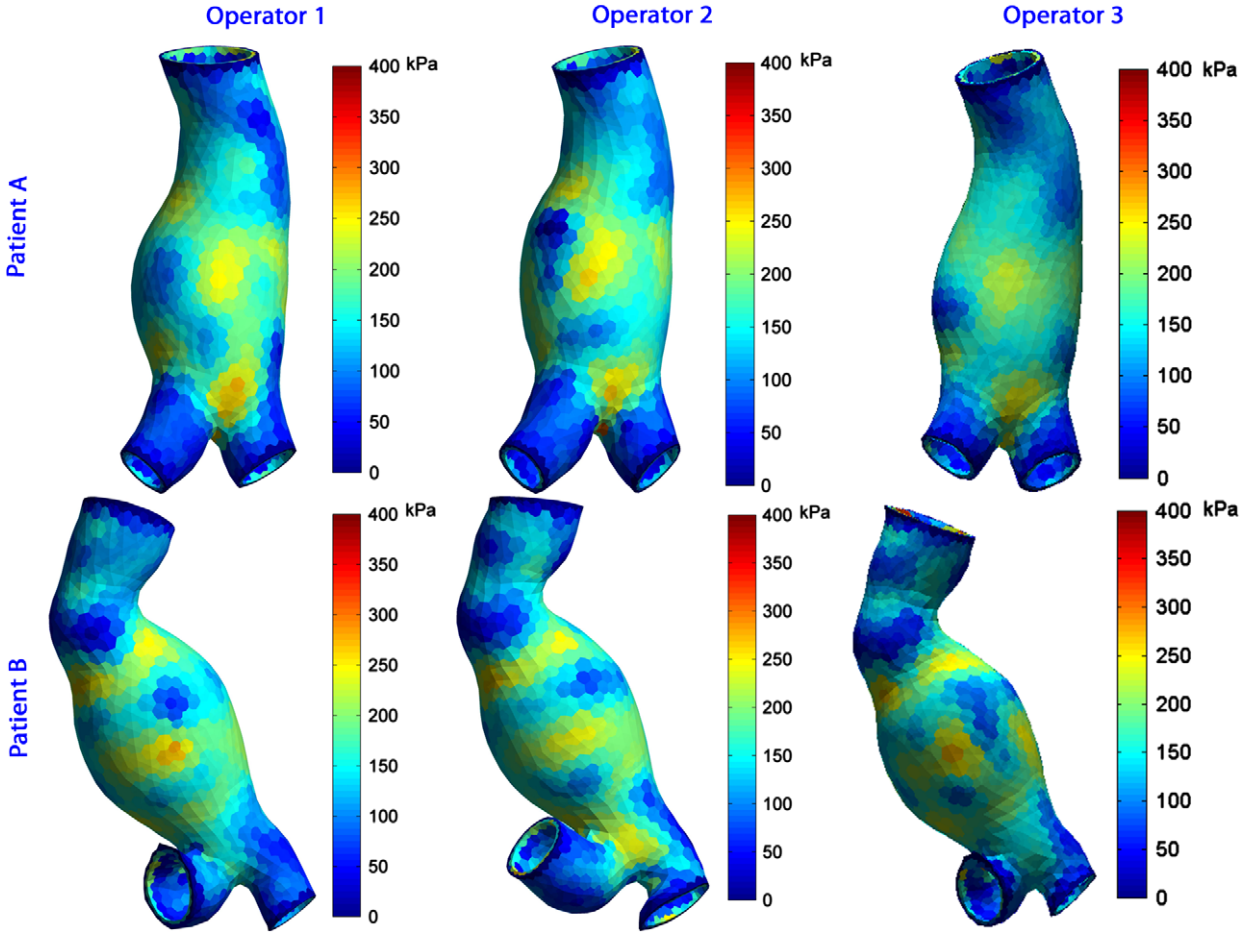

Figure 3 Posterior view of the stress distributions for two patients for operators 1, 2 and 3.

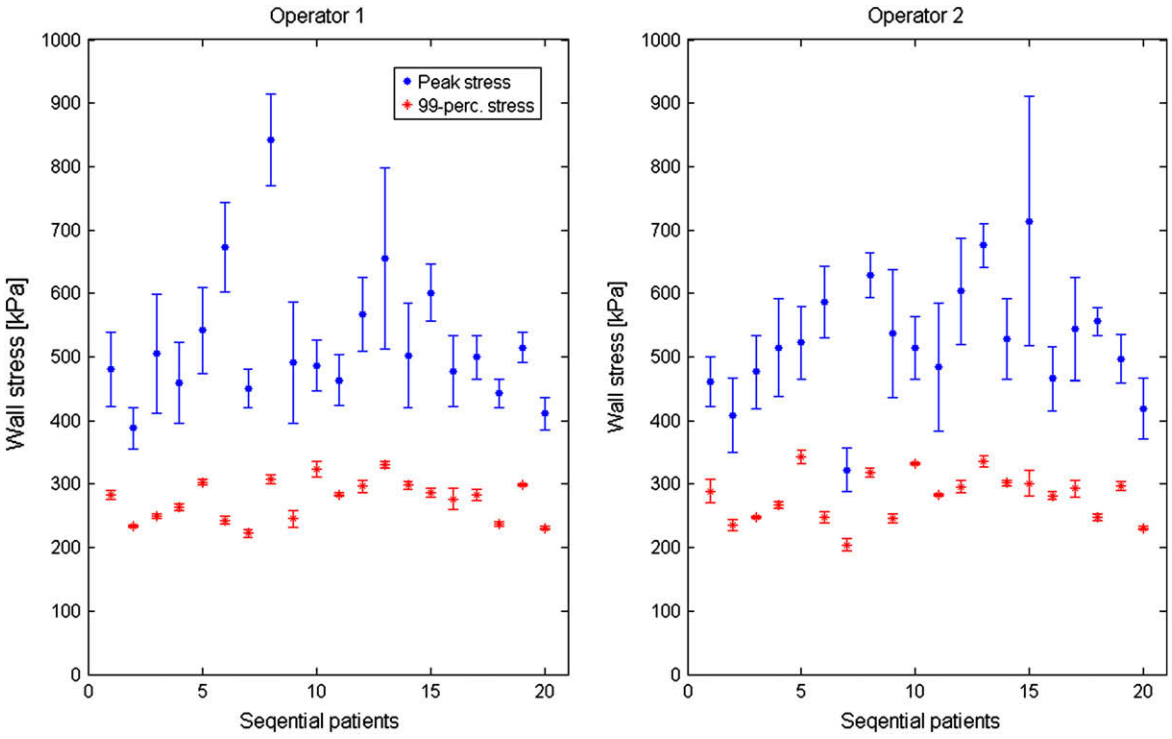

Figure 4 The mean and standard deviation of the peak stress and 99-percentile stress for the 5 analyses of all patients as determined by operator 1 (left) and 2 (right).

Wall stress analysis

In the simulations, the patient group averaged SP of 140 mmHg (18.7 kPa) was used as input pressure. The time required to segment an AAA once was 10 min on average. None of the twenty AAA segmentations were completely rejected, although two AAAs were segmented without aortic bifurcation. Manual adaptations of slice contours were required for almost all AAAs to correct 3DAO ingrow in either the vena cava or other surrounding tissues. The computations took approximately 1 h on average per geometry.

Fig. 3 displays the wall stress distributions for one segmentation of two patients, for the three operators. The location of the peak stress was identified for all performed segmentations (in total 220). Only a few AAA models showed a peak stress on one of the boundaries, resulting from the applied boundary conditions (10 or 5%). The rest had the peak stress situated either at the aortic bifurcation (98 or 45%) or at the beginning (45 or 20%) or end (67 or 30%) of the dilation.

Intra-operator variability

The mean and standard deviation of the peak and 99-percentile stress for all patients are given in Fig. 4 for both operators separately.

The average standard deviation as a percentage of the mean for the peak stress is 11% (operator 1, range 5—22%) and 12% (operator 2, range 4—28%), whereas for the 99-percentile stress it is 2% (operator 1, range 1—6%) and 3% (operator 2, range 1—7%). The intra-operator ICC for operator 1 was 0.73 for peak stress and 0.94 for 99-percentile stress. For operator 2 this was 0.79 and 0.94, respectively.

The absolute differences between the first two and the last two segmentations were not significantly different for the peak and 99-percentile stress (p-value 0.19 and 0.43 for operator 1 and 0.33 and 0.84 for operator 2), indicating that no learning curve could be identified.

Inter-operator variability

The number of manual adaptations was not tracked automatically, but all operators indicated that 2—5 adaptations were made in each AAA. The inter-operator ICC was 0.71 for the peak wall stress and 0.95 for 99-percentile stress. Fig. 5 shows the Bland—Altman plots for the peak stress and the 99-percentile stress, comparing all operators mutually. The mean differences ($\pm$SD) between all operators are given in Table 2. From this it becomes clear that the average peak and 99-percentile stress for operator 3 is lower than operator 1 and on his turn lower than operator 2. The average differences are however small compared to the average stress values. The standard deviation for the differences in peak stress is 76 kPa on average, which is about 15% of the average peak wall stress. For the 99-percentile stress, the average standard deviation is 10 kPa, which is less than 4% of the average 99-percentile stress.

Geometrical parameters

To evaluate the relation between the AAA diameter and the stress estimates, first the stress estimates per patient are averaged over all operators. A simple regression analysis

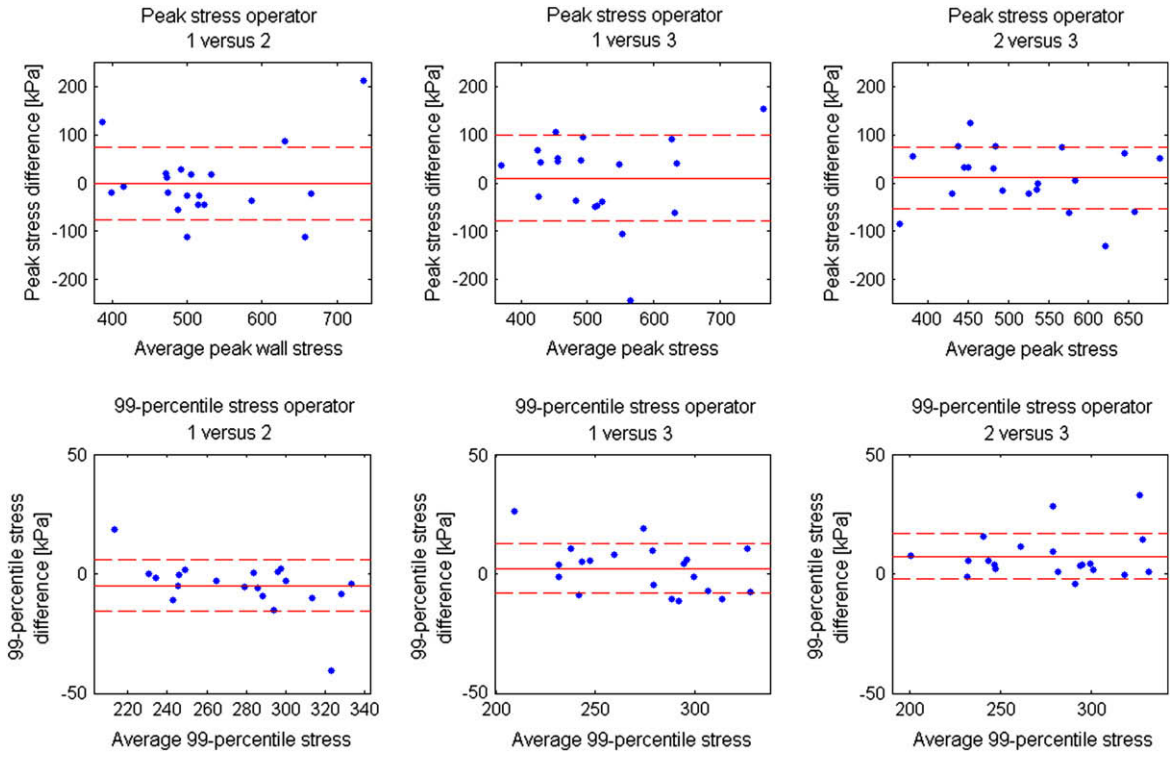

Figure 5 Bland–Altman plots for operators 1, 2 and 3 (- - indicates one standard deviation).

did not lead to a significant relationship between the peak wall stress and the maximum diameter (p-value 0.19). Fig. 6 shows the linear regression model between the operator-averaged 99-percentile stress and the maximum diameter (left, $R^2 = 0.75$, p-value < 0.001). The residuals between the computed stresses and the regression model are normalized by the standard deviation of the residuals and plotted on the right in Fig. 6. Five AAAs have stresses more than one standard deviation above the predicted regression model (A–E). Four AAAs have values more than one standard deviation beneath the model (F–I).

Fig. 7 A–I shows the geometries of the outliers. Table 3 displays the average tortuosity (±SD) of the CLL and CFL for the high, normal and low stress AAAs. Although not significant, the tortuosity for the high stress AAAs is larger than for the normal stress AAAs and the low stress AAAs. No significant differences were found between the tortuosity of the CLL and CFL.

Discussion

Although the operators in this study all have different experience with the segmentation procedure and with reading CT-data of AAA patients, they all were easily familiarized with the software and all found it easy and intuitively to use. This indicates that an easy transition into the clinic is possible once the software has proven to be of significant value in the AAA rupture risk analysis.

Fig. 3 shows that the stress distributions as derived from the segmentations of each operator show strong similarities. Only in a small selection of models (5%), the peak stress was caused by the applied boundary conditions. No effort was therefore made to eliminate the stresses at the boundaries of the models or to apply more advanced boundary conditions. Due to the small number of patients in this study, no conclusions could be drawn about the location of peak wall stress. A future study may elaborate on this in relation to the site of rupture. The location of the 99-percentile stress could not be determined as this stress value is not unique, but can occur on multiple locations on the AAA wall.

Small subtle shape changes induced by the segmentation of different operators, however, appear to influence the magnitude of the stress estimates. The intra-operator ICC for the peak stress was 0.73 for operator 1 and 0.79 for operator 2 and 0.94 for the 99-percentile stress for both operators. Heng et al. found an intra-operator ICC for the peak stress of 0.84, which is in the same range as our findings for the peak stress, but inferior to the correlation for 99-percentile stress.[9] No learning effect could be found for both operators, which indicates that the automatic software is insensitive to the experience and training of the user.

Table 2 Mean differences (±standard deviation) between all operators for peak and 99-percentile of stress

	Operator 1–2	Operator 1–3	Operator 2–3
Peak stress (kPa)	-0.2 ± 75.5	10.4 ± 89.4	10.6 ± 63.5
99-Percentile of stress (kPa)	-5.0 ± 10.8	2.3 ± 10.3	7.3 ± 9.5

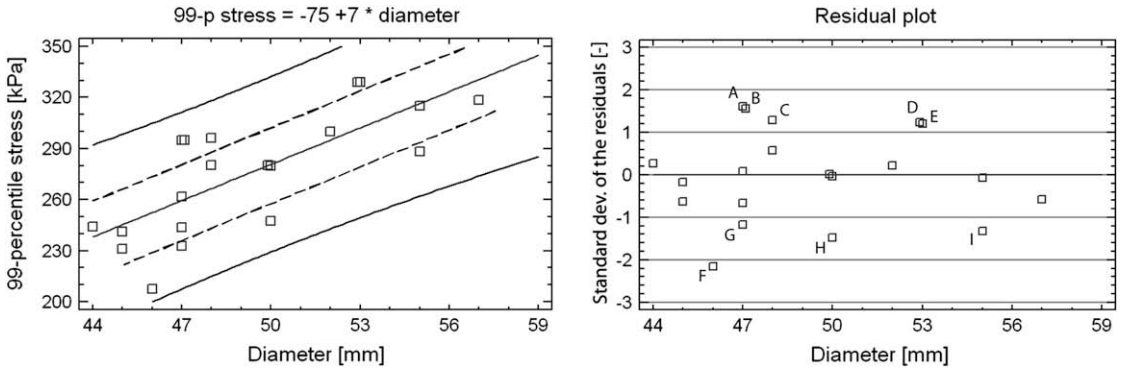

Figure 6 Linear regression between the 99-percentile stress and the maximum diameter (left, - - indicates one standard deviation) and the residuals of the regression model, normalized to the standard deviation of the residuals (right).

The inter-operator ICC for the peak stress was 0.71 which was identical to the findings by Heng et al.[9] For the 99-percentile stress, an inter-operator ICC of 0.95 was found. The 99-percentile stress is therefore less sensitive to the type of user and their experience. Reproducibility was compared between patients with a CT-scan with 1 and 2 mm slices and for different sub-groups within our patient selection (male/female, smoking/non-smoking and hypertensive/normotensive). No difference in reproducibility in wall stress was found for each of the parameters. A future study based on a larger patient population may elaborate more on this subject.

Subsequently, a regression model was fitted to both the peak and 99-percentile stress as a function of the diameter (Fig. 6). No significant relation between peak wall stress and the maximum diameter could be found for the 20 AAAs in this study. For the 99-percentile stress, a linear relation was found with a moderate regression coefficient ($R^2 = 0.75$).

Nine outliers were identified outside one standard deviation of the residuals from the regression model. The tortuosity of the CLL and CFL was not significantly different in any of the three groups (Table 3). Pappu et al. observed previously that an increased aortic tortuosity might be associated with increased rupture risk.[17] Fillinger et al. on the other hand, found a greater risk for AAAs with no or mild tortuosity.[15] The present study cannot give clear evidence that could favor one of the two assumptions on tortuosity and increased risk. A larger patient population is required to further investigate the relation between tortuosity or other geometrical features and AAA wall stress.

In this study, also lower percentiles stress were assessed. The inter-operator ICC of the 95-percentile stress was slightly better than for the 99-percentile stress (0.97 versus 0.95), however, differences between patients were also smaller, leading to a lower discriminatory power. Future research may include a parameter study to find the

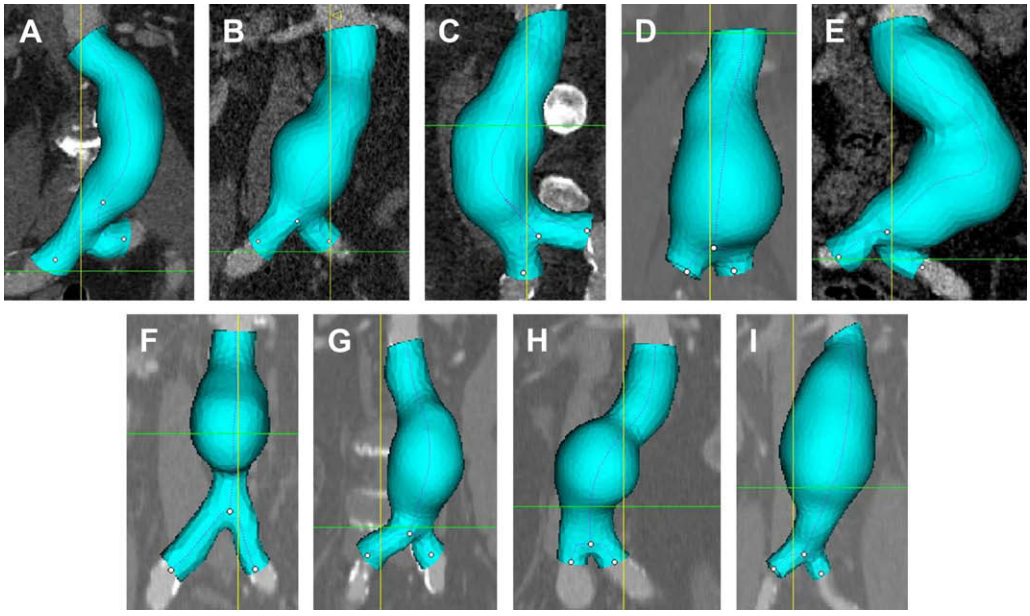

Figure 7 A—E 'high stress AAAs' with stresses more than one standard deviation above the regression model. F—I 'low stress AAAs' with stresses below the regression model.

Table 3 Tortuosity of the central lumen and flow line for high, normal and low stress AAAs

	Tortuosity	
	Central lumen line	Central flow line
High stress ($n = 5$)	1.66 ± 0.49	1.67 ± 0.68
Normal stress ($n = 11$)	1.44 ± 0.19	1.21 ± 0.21
Low stress ($n = 4$)	1.33 ± 0.09	1.19 ± 0.12

percentile with the best ratio between intraclass correlation and discriminatory power.

This study has a number of limitations that may have influenced the results. Wall stress simulations in this study are all performed with a linear material model. Extending the current wall stress simulation with the non-linear material model that is proposed by Raghavan and Vorp[18] may have an effect on the reproducibility results. This effect will however become apparent in both the peak and 99-percentile stress and we believe that this will not influence the conclusions of the present study. Future adaptations to our procedures will be made to compare the effect of a more complex material model for the AAA wall.

Additionally, the choice of a constant wall thickness is a significant and inevitable limitation. It is known that local wall thickness may strongly vary within AAAs, which may strongly influence the wall stresses.[19] However, non-invasive methods to measure local wall thickness are currently unavailable.

Initial stresses are caused by the pressure acting on the AAA during imaging, and are not accounted for in the wall stress simulations. Lu et al. studied the effect of initial stresses and concluded that the peak wall stress is overestimated, when initial stresses are not accounted for.[20] This would again affect both the reproducibility of the peak and 99-percentile wall stress and therefore we believe that it does not influence the conclusions. Taking into account the initial stresses however does improve the accuracy of the model and incorporating initial stresses in our methods is currently under investigation.

No intraluminal thrombus (ILT) was incorporated in the wall stress simulations as it was believed that the soft ILT tissue[21] propagates the intra-aortic pressure in a fluid-like fashion, and hardly influences the wall stress results. This is supported by intra-thrombus pressure measurements by Schurink et al. on the AAAs of 9 patients during open repair.[22] Additionally, calcifications were not incorporated in the models, although we previously showed the significant effect that these calcium deposits may have on the wall stress.[23] Others defined the role of calcium deposits in rupture risk of AAAs.[24] The automatic procedures in this study, however, do not facilitate the determination and application of calcifications in the finite element models. Currently, our methods are extended with the option of incorporating ILT and calcifications in the wall stress analysis.

Conclusion

The relative low intraclass correlations of the peak wall stress, found in this and previous[9] research, limits the suitability of peak stress as reliable wall stress parameter. The 99-percentile stress proves to have a much higher reliability, by being insensitive to small geometrical variations and to the background and experience of the operator. The maximum diameter showed a strong relation with the wall stress. AAAs with stresses outside this relation could not be discriminated by the tortuosity of the AAA.

Acknowledgements

The authors would like to thank Steven Koppelman for his important contribution to this work as operator and Ursula Kose (Philips Medical Systems, Best, The Netherlands) for her software implementation.

References

1 Greenhalgh RM, Forbes JF, Fowkes FG, Powel JT, Ruckley CV, Brady AR, et al. Early elective open surgical repair of small abdominal aortic aneurysms is not recommended: results of the UK small aneurysm trial. Steering committee. *Eur J Vasc Endovasc Surg* 1998;**16**(6):462–4.
2 Darling RC, Messina CR, Brewster DC, Ottinger LW. Autopsy study of unoperated abdominal aortic aneurysms. The case for early resection. *Circulation* 1977;**56**(Suppl. 3):II161–4.
3 Nicholls SC, Gardner JB, Meissner MH, Johansen HK. Rupture in small abdominal aortic aneurysms. *J Vasc Surg* 1998;**28**(5):884–8.
4 Vorp DA, Vande Geest JP. Biomechanical determinants of abdominal aortic aneurysm rupture. *Arterioscler Thromb Vasc Biol* 2005;**25**(8):1558–66.
5 Fillinger MF, Raghavan ML, Marra SP, Cronenwett JL, Kennedy FE. In vivo analysis of mechanical wall stress and abdominal aortic aneurysm rupture risk. *J Vasc Surg* 2002;**36**(3):589–97.
6 Venkatasubramaniam AK, Fagan MJ, Mehta T, Mylankal KJ, Ray B, Kuhan G, et al. A comparative study of aortic wall stress using finite element analysis for ruptured and non-ruptured abdominal aortic aneurysms. *Eur J Vasc Endovasc Surg* 2004;**28**(2):168–76.
7 Raghavan ML, Fillinger MF, Marra SP, Naegelein BP, Kennedy FE. Automated methodology for determination of stress distribution in human abdominal aortic aneurysm. *J Biomech Eng* 2005;**127**(5):868–71.
8 Truijers M, Pol JA, Schultzekool LJ, van Sterkenburg SM, Fillinger MF, Blankensteijn JD. Wall stress analysis in small asymptomatic, symptomatic and ruptured abdominal aortic aneurysms. *Eur J Vasc Endovasc Surg* 2007;**33**(4):401–7.
9 Heng MS, Fagan MJ, Collier JW, Desai G, McCollum PT, Chetter IC. Peak wall stress measurement in elective and acute abdominal aortic aneurysms. *J Vasc Surg* 2008;**47**(1):17–22.
10 De Putter S, Breeuwer M, Vosse F van de, Kose U, Gerritsen FA. Patient-specific models of wall stress in abdominal aortic aneurysm: a comparison between MR and CT. In: Proceedings of SPIE medical imaging, vol. 6143; 2006. p. 61430D1–12.
11 De Putter S, Breeuwer M, Kose U, Laffargue F, Rouet J-M, Hoogeveen R, et al. Automatic determination of the dynamic geometry of abdominal aortic aneurysm from MR with application to wall stress simulations. In: Proceedings of the 19th international computer assisted radiology and surgery conference. Berlin, Germany; 2005;339–344.
12 Delingette H. Modélisation, Déformation et Reconnaissance d'objets tridimensionnels a l'aide de maillages simplexes. PhD thesis, Ecole Centrale de Paris; 1994.

13 Gérard O, Collet Billon A, Rouet J-M, Jacob M, Fradkin M, Allouche C. Efficient model-based quantification of left ventricular function in 3-D echocardiography. *IEEE Trans Med Imaging* 2002;**21**:1059—68.
14 Ollabarriaga SD, Rouet J-M, Fradkin M, Breeuwer M, Niessen WJ. Segmentation of thrombus in abdominal aortic aneurysms from CTA with non-parametric statistical grey level appearance modeling. *IEEE Trans Med Imaging* 2005;**24**:477—85.
15 Fillinger MF, Racusin J, Baker RK, Cronenwett JL, Teutelink A, Schermerhorn ML, et al. Anatomic characteristics of ruptured abdominal aortic aneurysm on conventional CT scans: implications for rupture risk. *J Vasc Surg* 2004; **39**(6):1243—52.
16 Chaikof EL, Fillinger MF, Matsumura JS, Rutherford RB, White GW, Blankensteijn JD, et al. Identifying and grading factors that modify the outcome of endovascular aortic aneurysm repair. *J Vasc Surg* 2002;**35**(5):1061—6.
17 Pappu S, Dardik A, Tagare H, Gusberg RJ. Beyond fusiform and saccular: a novel quantitative tortuosity index may help classify aneurysm shape and predict aneurysm rupture potential. *Ann Vasc Surg* 2008;**22**(1):88—97.
18 Raghavan ML, Vorp DA. Towards a biomechanical tool to evaluate rupture potential of abdominal aortic aneuryms: identification of a finite strain constitutive model and evaluation of its applicability. *J Biomech* 2000;**33**(4):475—82.
19 Thubrikar MJ, al-Soudi J, Robicsek F. Wall stress studies of abdominal aortic aneurysm in a clinical model. *Ann Vasc Surg* 2001;**15**(3):355—66.
20 Lu J, Zhou X, Raghavan ML. Inverse method of stress analysis for cerebral aneurysms. *Biomech Model Mechanobiol*; 2007 Nov 8 [Epub ahead of print].
21 van Dam EA, Dams SD, Peters GW, Rutten MC, Schurink GW, Buth J, et al. Non-linear viscoelastic behavior of abdominal aortic aneurysm thrombus. *Biomech Model Mechanobiol* 2008; **7**(2):127—37.
22 Schurink GW, van Baalen JM, Visser MJ, van Bockel JH. Thrombus within an aortic aneurysm does not reduce pressure on the aneurysmal wall. *J Vasc Surg* 2000;**31**(3):501—6.
23 Speelman L, Bohra A, Bosboom EM, Schurink GW, van de Vosse FN, Makaroun MS, et al. Effects of wall calcifications in patient-specific wall stress analyses of abdominal aortic aneurysms. *J Biomech Eng* 2007;**129**(1):105—9.
24 Siegel CL, Cohan RH, Korobkin M, Alpern MB, Courneya DL, Leder RA. Abdominal aortic aneurysm morphology: CT features in patients with ruptured and nonruptured aneurysms. *Am J Roentgenol* 1994;**163**:1123—9.